Searches for Exotic Particles at Tevatron

Amber Boehnlein
For the CDF and DØ Collaborations
ms234 Fermi National Accelerator Laboratory, Batavia, IL 60510

Searches for new particles have been conducted at the Tevatron using data from the 1992–1996 data sets. Brief descriptions of searches for vector leptoquarks, Dirac monopoles and technicolor particles are presented here.

1 Introduction

The CDF and DØ collaborations, working with data from the 1992–96 Fermilab Tevatron $\bar{p}p$ collider runs, have a broad program to search for new physics. In many cases, the two experiments are complementary either in search method or in analysis as both CDF[1] and DØ[2] are well designed for new particle searches. A sampling of the most recent results is briefly presented.

2 Searches for Vector Leptoquarks

Leptoquarks (LQ) are found in many extensions of the Standard Model and would be color-triplet bosons that couple to quarks and leptons and can be either scalar or vector particles[3]. Leptoquarks have to be either very massive or couple only within a single generation to be consistent with flavor-changing neutral current constraints[4]. Leptoquarks would be produced at the Tevatron primarily through $q\bar{q}$ anhiliation and gluon fusion, and the cross section does not depend on the unknown $LQ - l - q$ coupling. They could decay to a charged lepton-quark pair (lj) or a ν-quark pair (νj). The branching fraction β is defined to be 1 when all LQs decay to lj, and 0 when all LQs decay to νj. Since LQ are produced in pairs at the Tevatron, there are three possible final states for each generation. CDF and DØ have searched for LQ production in all three generations[5,6,7,8,9] and these results are summarized in Table 1.

Vector leptoquarks (VLQ) can behave as gauge bosons or as composite particles with anomalous couplings. The cross section depends on the coupling, but is generally higher than scalar LQ production because of the spin. The parameters κ and λ are the anomalous coupling parameters of the leptoquarks to the gluon fields which determine the magnitude of the destructive interference between the production diagrams. No anomalous coupling, referred to as Yang-Mills coupling ($\kappa = 0, \lambda = 0$) gives the maximum vector leptoquark cross section. The anomalous coupling case with $\kappa = 1, \lambda = 0$ has the minimal vector coupling, while $\kappa = 1.3, \lambda = -0.2$ leads to the minimum vector cross section. DØ has searched for first generation vector leptoquarks, having shown that the kinematic distributions for scalar and vector leptoquarks are similar enough that the optimization from the scalar LQ search can be used. The cuts, analysis methods, and data samples are described in detail elsewhere [5,6,10]. Vector LQ Monte Carlo samples were generated using a modified version of PYTHIA[11,12]. Fig. 1, left panel, shows the

Table 1: Summary of current Tevatron leptoquark mass limits

Collaboration	β	Channel	Mass Limit
First Generation Scalar			
CDF	1	$eejj$	213 GeV/c^2
CDF	$\frac{1}{2}$	$e\nu jj$	180 GeV/c^2
DØ	1	$eejj$	225 GeV/c^2
DØ	$\frac{1}{2}$	$eejj$ and $e\nu jj$	204 GeV/c^2
DØ	0	$\nu\nu jj$	79 GeV/c^2
Tevatron	1	$eejj$	242 GeV/c^2
Second Generation Scalar			
CDF	1	$\mu\mu jj$	197 GeV/c^2
CDF	$\frac{1}{2}$	$\mu\mu jj$	133 GeV/c^2
DØ	1	$\mu\mu jj$	184 GeV/c^2
DØ	$\frac{1}{2}$	$\mu\mu jj$	140 GeV/c^2
Third Generation Scalar			
CDF	1	$\tau\tau jj$	99 GeV/c^2
DØ	0	$\nu\nu bb$	94 GeV/c^2
Third Generation Yang-Mills Vector			
CDF	1	$\tau\tau jj$	225 GeV/c^2
DØ	0	$\nu\nu bb$	216 GeV/c^2

exclusion contours in the plane of M_{VLQ} vs. β for the VLQ analysis for each of the three decay channels and the combined limit for the Yang-Mills coupling. The $eejj$ channel has maximum exclusion at $\beta = 1$, the $\nu\nu jj$ channel at $\beta = 0$ and the $e\nu jj$ channel at $\beta = 1/2$. The right panel of Fig. 1 shows the effects on the combined limit of the choice of different VLQ couplings, with the three cases shown described as above. The lower limits on the mass of a first generation vector leptoquark with Yang-Mills coupling are (340, 325, 200) GeV/c^2 for $\beta = (1, \frac{1}{2}, 0)$. For the minimal vector coupling case, the lower limits on the vector leptoquark mass are (290, 275, 145) GeV/c^2 for $\beta = (1, \frac{1}{2}, 0)$. The minimum vector leptoquark cross section case leads to lower limits on the vector leptoquark mass of (245, 230, 145) GeV/c^2 for $\beta = (1, \frac{1}{2}, 0)$.

3 A Search for Heavy Pointlike Dirac Monopoles

Magnetic monopoles were introduced by P. Dirac [13] to symmetrize Maxwell's equations and explain the quantization of electric charge. Searches for monopoles in cosmic rays for the relic monopole flux are not sensitive to the monopole mass. L3 [14] has searched for monopoles in $Z \to \gamma\gamma\gamma$ leading to a lower limit on the monopole mass of 510 GeV/c^2. Dirac monopoles would be expected to couple to photons with an effective coupling constant $\alpha_g = g^2/4\pi$ where g is the magnetic charge, and is related to the electric charge e, $g = 2\pi n/e$ where n is an unknown, non-zero integer. The monopoles could give rise to photon-photon rescattering, and the contribution of this process to diphoton production at the Tevatron [15] has been calculated. The signature for this low Q^2 process is two high E_T photons that are generally centrally produced and no additional particles in the event. The DØ collaboration has searched for pointlike Dirac monopoles[16] in a study based on 69.5 $\pm$ 3.7 pb^{-1} of data collected on a trigger which did not require the presence of an inelastic collision. The initial event selection is two or more photons with E_T> 40 GeV and pseudorapidity $|\eta^\gamma| < 1.1$; no significant missing transverse energy $\not{E}_T$< 25 GeV; and no jets with $E_T^j > 15$ GeV and $|\eta^j| < 2.5$. This leads to an initial data

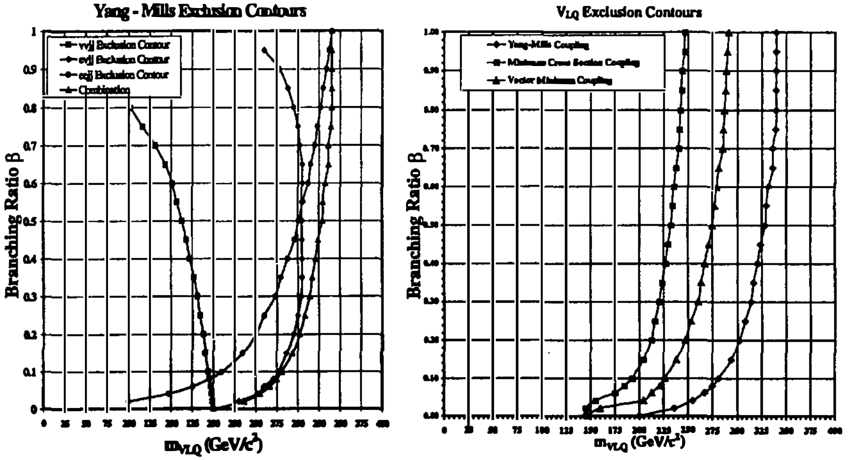

Figure 1: Left: The 95% CL exclusion contour in the plane of M_{VLQ} vs. β for the case of Yang-Mills coupling. The exclusion for the $eejj$ channel is shown as circles; $e\nu jj$ channel as diamonds; for the $\nu\nu jj$ channel as squares. The combined limit from all three channels is shown as triangles.
Right: The 95% CL exclusion contour combined for all three channels shown for three different choices of λ and κ: The Yang-Mills coupling is shown as diamonds; Minimum Vector coupling shown as triangles; Minimum Vector cross section shown as boxes. These results are preliminary.

sample of 90 candidate events, with a predicted background of 88 $\pm$ 12 events, primarily from Drell-Yan processes where the electron tracks were not reconstructed and from multijet sources in which jets are misidentified as photons. Backgrounds from photon-photon rescattering due to a virtual W-loop have been shown to be small[17].

To enhance the signal relative to the background, optimisation was performed by varying $S_T^\gamma = \sum E_T^\gamma$ until the expected background was 0.4 events. The final selection is $S_T^\gamma > 250$ GeV, leading to no events observed in the data sample and an expected background of 0.41 $\pm$ 0.11 events. The overall acceptance of the kinematic cuts for the monopole signal is (51 $\pm$ 1)%, while the efficiency of the particle identification cuts is (52.8 $\pm$ 1.4)%. The acceptance and efficiency are independent of monopole mass. The upper limit for the production cross section of two or more photons with this selection is $\sigma(p\bar{p} \to \geq \gamma\gamma) < 83$ fb. This limit is represented on Fig. 2 as a horizontal line.

The heavy monopole production cross section at the Tevatron is given by:[15]

$$\sigma(p\bar{p} \to \gamma\gamma + X) = 57P(S)(n/M[\mathrm{TeV}])^8 \text{ fb}$$

where P(S) is a spin dependent factor. The estimated error on this cross section due to the choice of p.d.f. and to higher order QED effects is 30%. The theoretical cross sections are represented on Fig. 2 as bands corresponding to three spin cases. Arrows on Fig. 2 represent the 95% CL lower limit on M/n for the three spin cases and correspond to

$$\begin{aligned} M/n &> 610 \text{ GeV/c}^2 \text{ for S} = 0 \\ M/n &> 870 \text{ GeV/c}^2 \text{ for S} = 1/2 \\ M/n &> 1580 \text{ GeV/c}^2 \text{ for S} = 1. \end{aligned}$$

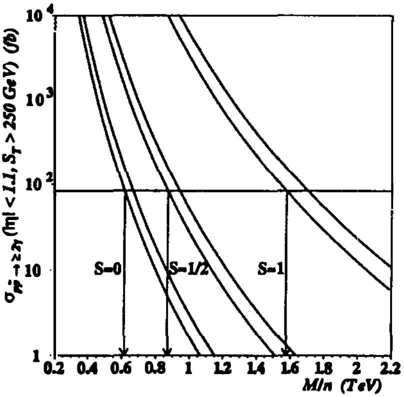

Figure 2: The curved bands show the lower and upper bounds on the theoretical cross sections[18] for monopole spin, S = 0, 1/2, and 1. The horizontal line shows the 95% CL experimental upper limit[16] on the cross section. The arrows indicate the lower 95% CL limits on the monopole mass at each spin value as a function of M/n

4 Searches for Technicolor

Technicolor theories provide a dynamical explanation for electroweak symmetry breaking. In recent work, Extended Technicolor models[18,19] have been constructed that lead to a rich particle spectrum accessible at Tevatron energies. Light, color-singlet technipions (π_T) have Higgs-like coupling to fermions, with $\pi_T^+ \to b\bar{c}, c\bar{s}, \tau\nu_\tau$ and $\pi_T^0 \to b\bar{b}$. The technivector mesons, the isotriplet ρ_T and isoscalar partner ω_T are expected to have equal masses as techni-isospin is an approximate symmetry. Walking Technicolor could enhance the mass of the π_T, possibly closing the channels $\rho_T \to \pi_T\pi_T$ and $\omega_T \to \pi_T\pi_T\pi_T$. The decay modes $\rho_T \to W_L\pi_T$ and $\rho_T \to Z_L\pi_T$ and $\omega_T \to \gamma\pi_T$ might then dominate, leading to distinctive experimental signatures with heavy flavor tagged jets.

The ω_T is produced via vector-meson dominance with a cross section that is proportional to $|Q_u + Q_d|^2$, where Q_u and Q_d are the electric charges of the constituent technifermions [18]. CDF has searched for ω_T production in a final state with a photon with $E_T > 25$ GeV and $|\eta| < 1.0$ and two jets with $E_T > 30$ GeV and $|\eta| < 2.0$ where one of the jets is associated with a b tag in the silicon vertex detector. In this initial sample, 200 events are observed in 85 pb^{-1} with a predicted background of 131 $\pm$ 30 $\pm$ 29 events. The background sources are photons produced with heavy flavor, photon events with a misidentified tag and misidentified photon events. Since all particles are reconstructed, the π_T would appear as a resonance in the invariant mass of the dijet pair $M(bj)$, and ω_T would appear as a resonance in the three particle invariant mass $M(\gamma bj)$. A target π_T mass $\pm$ 40 GeV/c^2 window determines the sample to be fit for a series of ω_T mass hypotheses. For events in the π_T mass window, the mass difference $M(\gamma bj) - M(bj)$ is fit using a binned likelihood method. A gaussian distribution is assumed for the signal and two models are used to describe the background, a single or the sum of two exponential distributions. To be conservative, the fit that results in the worse limit is used to set the 95% CL upper limit on the cross section. The experimental limit is compared to the

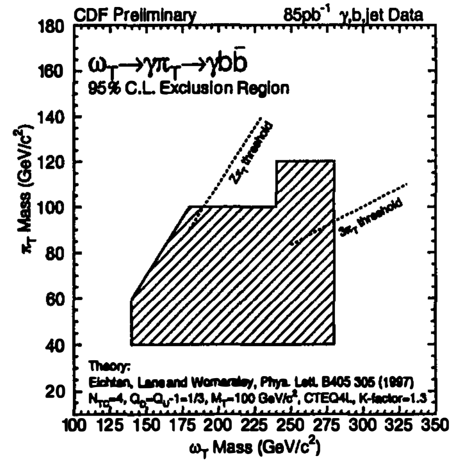

Figure 3: M_{ω_T} vs. M_{π_T} exclusion contour is shown as the cross hatched region. The model parameters [18] are four technicolors, $Q_u = 4/3$, and $M_T = 100$ GeV/c^2. The kinematically allowed regions for the channels $\omega_T \to Z\pi_T$ and $\omega_T \to \pi_T\pi_T\pi_T$ are indicated by dashed lines. These results are preliminary.

theoretical cross section in a model [18] with four technicolors, $Q_u = 4/3$ and $Q_d = 1/3$ and the mass parameter $M_T = 100$ gevcc. The exclusion contour for this model in the plane of the M_{ω_T} vs. M_{π_T} is shown in Fig. 3 as the cross hatched region. In the model considered, ω_T masses from 130 GeV/c^2 to 280 GeV/c^2 are excluded for $M_{\pi_T} = 40$ GeV/c^2, while π_T masses from 40 GeV/c^2 to 120 GeV/c^2 are excluded for $M_{\omega_T} = 280$ GeV/c^2. For this analysis, the branching fractions of $\omega_T \to Z\ \pi_T$ and $\omega_T \to \pi_T\pi_T\pi_T$ are assumed to be negligible. Dashed lines on Fig. 3 indicate the kinematically allowed regions for those decays.

CDF has also searched for the production of ρ_T via vector meson dominance in the decay modes $\rho_T{}^{\pm} \to W_L\pi_T{}^0$ and $\rho_T{}^0 \to W_L\pi_T{}^{\pm}$ with the π_T decaying to jets, one with a c or b quark tag and the W_L decaying to $l\nu$. The preliminary event selection requires an electron or muon with $p_T > 20$ GeV and $|\eta| < 1.1$, $\not{E}_T > 20$ GeV, and two jets with $E_T > 20$ GeV and $|\eta| < 2.0$ where one of the jets is required to have a heavy flavor tag in the silicon vertex detector. This selection leads to 42 events observed in 109 pb^{-1} with a predicted background of 31.6 ± 4.3 events from W boson production and Top quark production. In the signal search region under consideration, $M_{\pi_T} + M_{W_L} \approx M_{\rho_T}$. Thus for the signal, the π_Ts are produced nearly at rest and topological cuts can be placed on the difference between the azimuthal angles of the two jets $\Delta\phi(jj)$, and the transverse momentum of the dijet system $p_T(jj)$. The values of these cuts are chosen to maximize $S/\sqrt{B}$ for each signal sample. Finally a sliding mass window cut is applied, using target masses $\pm 3\sigma$ for the π_T ($M(jj)$) and the ρ_T ($M(Wjj)$). The systematic uncertainty in the signal efficiency is 26%. The 95% CL upper limit on the cross section is calculated for each point in π_T, ρ_T mass, and compared to the theoretical cross section calculation [19] to obtain the exclusion contour as shown in the dark area of Fig. 4. This analysis excludes ρ_T masses in a range from 178 GeV/c^2 to 192 GeV/c^2, for $M_{\pi_T} = 95$ GeV/c^2. In addition, Fig. 4 also shows lines corresponding to constant production cross sections, giving an indication of the sensitivity to the production of techniparticles with a larger data set.

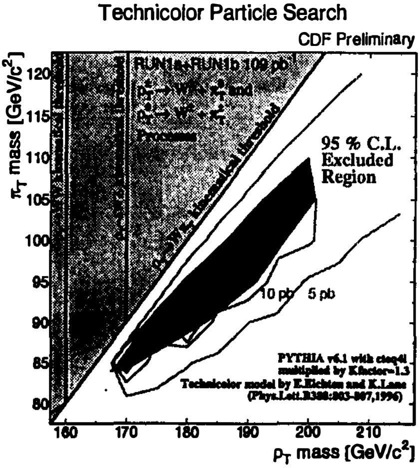

Figure 4: The 95% CL exclusion contour in the plane of M_{ρ_T} vs M_{π_T} is shown as the dark area. These results are preliminary. Lines corresponding to constant production cross sections[19] contours are shown for 5, 10, and 15 pb.

5 Conclusions

The Tevatron collider experiments will continue to examine the 1992–1996 data sets for new physics, as well as prepare for the next run with upgraded detectors and larger data sets. Both collaborations have invaluable experience and the rich and varied program of searches for new particles at CDF and DØ will continue to be pursued.

References

1. The CDF Collaboration, F. Abe et al., *Nucl. Instrum. Methods* **A271**, 387 (1988).
2. The DØ Collaboration, S. Abachi et al., *Nucl. Instrum. Methods* **A338**, 185 (1994).
3. J. .L Hewett and T. G. Rizzo, Phys. Rep. **183**, 193 (1989) and references therein.
4. M. Leurer, *Phys. Rev.* **D49**,333 (1994).
5. The DØ Collaboration, B. Abbott et al., *Phys. Rev. Lett.* **79** 4321 (1997).
6. The DØ Collaboration, B. Abbott et al., *Phys. Rev. Lett.* **80** 2051 (1997).
7. The DØ Collaboration, B. Abbott et al., accepted by *Phys. Rev. Lett.*.
8. The CDF Collaboration, F. Abe et al., *Phys. Rev. Lett.* **79** 4327 (1997).
9. The CDF Collaboration, F. Abe et al., *Phys. Rev. Lett.* **78** 2906 (1997).
10. The DØ Collaboration, S. Abachi et al., *Phys. Rev. Lett.* **76**, 2222 (1196).
11. T. Sjostrand, Comput. Phys. Commun. **82**, 74 (1994).
12. J. Blümlein, E. Boos, and A. Kryukov, Z. Phys. **C76**, 137 (1997).
13. P. A. M. Dirac, Proc. R. Soc. London, Ser. A 133, 60, 1931.
14. The L3 Collaboration, M. Acciarri et al., *Phys. Lett.* B345, 609 (1995).
15. I. F. Ginzburg and A. Schiller, submitted to *Phys. Rev.* D.
16. The DØ Collaboration, B. Abbott et al., submitted to *Phys. Rev. Lett.*.
17. G. Jikia and A. Tkabaladze, *Phys. Lett.* B323, 453, (1994).
18. E. Eichten, K. Lane and J. Womersley, *Phys. Lett.* B405, 305 (1997).
19. E. Eichten, and K. Lane, *Phys. Lett.* B388, 803 (1996).